SYNTHESIS OF ULTRAFINE POWDERS OF Nb-Al AND Nb-Si ALLOYS BY USING RF PLASMA REACTOR

T. Harada, T.Yoshida and K.Akashi
Department of Metallurgy and Materials Science, Faculty of Engineering,
The University of Tokyo, Hongo, Bunkyo-ku, Tokyo, 113 Japan.

ABSTRACT

Ultrafine powders of Nb-Al and Nb-Si alloys were synthesized by vaporization of a mixture of those components in an rf induced Ar plasma and the following condensation of the vaporized mixture under the tail flame of the plasma. The formation of $NbAl_3$ was confirmed by X-ray analysis of condensed ultrafine powders. Nb_5Si_3 was included in the product obtained from a mixed vapor of Nb-Si. Ultrafine powders of Nb_3Al and Nb_3Si have not been obtained.

1. INTRODUCTION

Ultrafine powders or particles (UFP) of various metals are generally produced by vaporization and condensation processes in an atmosphere of inert gas such as argon or helium. In the synthesis of UFP of an alloy consisted of various components, the control of its composition during the vaporization process is very difficult due to the difference between the vapor pressure of each component. The synthesis of UFP of Fe-Co-Ni(1), Fe-Pd(2), Ni-Pd, Au-Ni(3) and Cr-Ni(4) has been reported. However the vapor pressures of the components of these alloys are very similar as shown in Fig.1.. The formation of Fe-Al(2.2 wt%) solid solution from the vapor phase of Fe and Al at a quenching velocity of 10^4-10^5 K/sec has been reported(5).
In our study, the synthesis of UFP of Nb-Al and Nb-Si alloys was tried by vaporization and condensation processes using rf induced Ar plasma, though the vapor pressure of Nb was very different from that of Al or Si. Moreover, the effect of cooling velocity on the nucleation and growth mechanisms of UFP were analysed in connection with the experimental results.

2. EXPERIMENTAL

2-1. Preliminary Experiments

Fig.2. and Fig.3. are shematic diagrams of the rf plasma reactors(A) and (B) used for preliminary experiments to synthesize UFP of Nb-Al alloy. The reaction chamber is a stainless steel jacket in each reactor. The rf torch with a three turns rf coil is consisted of a tripple walled silica tube. The diameter of outer silica tube of the rf torch is about 50mm . The rf coil is consisted of tin-plated braided copper wires inserted into a three turns silica tibe. The cooling water is circulated through the silica tube. This silica tube resembles the rf coil of the reactor (C) used for main experiments as shown in Fig.7.
In main experiments for synthesis of UFP of Nb-Al and Nb-Si alloys, the reactors(C) and (D), as illustrated in Fig.4. and Fig.5., were used . In these cases, the diameter of outer silica tube is about 50mmϕ .

The reactor (C) was equipped with a copper quenching sphere for rapid cooling of vapor, which was placed at 12cm distance from the rf coil. In a few experiments, a water cooled radiation shield surrounding the quenching sphere was used as shown in Fig.6., but it was removed in most of experiments as shown in Fig.3.. In the reactor (D), the rf coil was consisted of two concentric silica tubes instead of three concentric silica tubes in other reactors and a water cooled copper coil was placed in a water cooled copper cup for condensation of vapor.
The upperpart of the chamber of the reactor (C) is made of pyrex glass. The detail of rf coil in the reactor (C) is shown in Fig.7.. The feed of powders into the rf torch was carried out from its both sides in the reactors (B) and (C). Starting materials were Nb powders of purity 99.5% with a diameter under 25 m, Al powders of purity 99.5% with a diameter under 25μm or 1μm (only in preliminary experiments) and Si powders of purity 99.99% with a diameter under 25 m, respectively. In all experiments, a powder feeder with a vibrator was used. The rf frequency and the maximum output power of the rf power generator were 4.0MHz and 30kw in both preliminary and main experiments. Nb and Al powders were mixed with an atomic ratio between 3:1 and 1:3 and introduced into the plasma with a carrier gas. The atomic ratio of Nb to Si for Nb-Si UFP preparation was 3:1. A product of UFP deposited on the water cooled substrate such as the quenching sphere of the cooling coil was examined by TEM and X-ray diffraction and chemical analysis.

RESULTS AND DISCUSSIONS

Typical experimental conditions in preliminary experiments using the reactor (A) and (B) are shown in Table 1.. It was estimated from changes of characteristic color of the plasma flame that the mixed powders of Al and Nb vaporized as soon as they were introduced into the plasma. The plasma was very stable at a larger feeding rate (0.3g/min.) of powders in the reactor (B) than that in the reactor (A). In main experiments, the reactor (C) was also operated stably with the supply of powders into the plasma from both sides of the rf coil. Nb, Nb_2Al and $NbAl_3$ were detected by X-ray diffraction analysis of the UFP obtained in several preliminary experiments. The grain size distribution of the UFP became narrow (several nm-50nm), when tha vapor phase was cooled rapidly with He gas injection from the quenching nozzle of the reactor (B). In these preliminary experiments, the existence of NbH phase was also confirmed in some products. This result means that H atoms permiate into Nb crystal lattice from the plasma including hydrogen. The UFP with NbH phase was annealed for 2 hrs. at 773K in vacuum of 10^{-6} Torr. The NbH phase disappeared and the lattice constant of Nb phase became shorter than that of pure Nb by 0.005A. Such reduction of the lattice may be due to the formation of Nb-Al solid solution by dissolution of Al atoms into Nb crystal lattice. The phase diagram of Nb-Al system is shown in Fig.8 (6). Nb has a certain degree of solubility of Al at room temperature.
In almost all of the main experiments, the powder feeding rate was maintained at 0.1g/min.. The experimental conditions are shown in Table 2. The results of X-ray diffraction analysis of the Nb-Al UFP are summarized in Table 3. Here the formation of $NbAl_3$ phase was confirmed. The X-ray diffraction chart of the UFP obtained from a mixture of Nb and Si powders with the atomic ratio of 3:1 is shown in Fig.9 , in comparison with that of arc-melted Nb-Si alloy with the atomic ratio of Nb:Si=3:1. It is expected from the phase diagram of Nb-Si system(7) that Nb_3Si and Nb_5Si_3 phases can be formed in the melted alloy. The broadening of X-ray diffraction lines from the Nb-Si UFP was observed, but the formation of Nb_5Si_3 (W_5Si_3 type) was confirmed. Fig.10 is a photograph of the UFP condensed on the quenching sphere of the reactor (C)

from the vapor of Nb and Si with the atomic ratio of 2;1. The mean diameter of the UFP is about 10nm. Sometimes spherical particles of Nb with diameters from several nm to hundreds nm were observed. the composition (Nb and Al contents) of the Nb-Al UFP and the mixture of Nb-Al (the starting material) were estimated by fluorescence X-ray analysis. The difference between the compositions of the two samples was only the order of 2%. The Nb-Al UFP was heated for 2 hrs at 1073K and 10^{-5}Torr. The X-ray diffraction lines from NbH phase disappeared and NbO phase was formed. NbO and NbO_2 were detected in the UFP of Nb obtained by using the reactor(D). It was considered from these results that oxygen took part in the formation of the oxides such as NbO and NbO_2.

The following experiments were carried out to confirm the difference among oxdizing behaviors of three kinds of samples, such as sample A (a mixture of Nb UFP and Al UFP made independently), Sample B (the UFP obtained from a mixture of Nb:Al with the atomic ratio of 3:1) and sample C (a finely divided alloy of arc-melted Nb-Si with the atomic ratio of 3:1). Each sample was oxidized completely by heating in a crucible. The formation of $NbAlO_4$ was confirmed in B and C samples, but not in sample A. Such facts suggest that Al can be in existence with Nb, even if the form of Al is not apparent.

Theoretical analyses of flow pattern and temperature distribution in the plasma tail flame adjoining the quenching sphere of the reactor(C) were tried, by applying the model of Gosman et al.(7), assuming the plasma as a thermal fluid of argon. The calculation were performed by using spherical co-ordinates for the shaded part as shown in Fig.11(a). The experiments were often carried out without such a water-cooled cover, but in these calculations, the cover was supposed to be on the quenching sphere to simplify boundary conditions. The dimensions of the range for the calculations are shown in Fig.11(b). Moreover the calculations were practiced under the following assumptions; 1. The plasma is a continuum of Ar. The effects of ionization and radiation can be neglected. 2. The pressure is latm in the whole range. 3. The steady state is established. 4. Local thermal equilibrium is established. The properties of Ar are given as functions of temperature. 5. The kinetic energy of fluid can be neglected, because it is smaller than its sensible heat in case of the calculation of temperature distribution. 6. Swirl velocity is regarded as 0.

The computer programmes are given by Harada(8). Fig.12 is an example of the results calculated on the following assumptions, that is, the maximum plasma temperature at the gas inlet of the cover along the center line of the plasma is 5273K, the gas velocity is $5m.sec^{-1}$ at the same point and the wall temperature is 773K. It can be estimated from this figure that the gas velocity decreases quickly near the surface of the quenching sphere. Therefore the cooling velocity of the vapor phase of Nb and Al cannot be considered to be sufficient for our experiments using the reactor (C). The cooling curves along two stream lines based on the results in Fig.12 are shown in Fig.13. From this figure, the cooling velocity is considered to be 10^4-10^5 $deg \cdot s^{-1}$.

There has been few experimental data about nucleation from metal's vapor. Kung et al(9) applied Lothe-Pound theory(10) to analyse the nucleation data of Fe. Here the nucleation temperatures of Nb, Si and Al calculated on Lothe-Pound theory were 3000, 2000 and 1500K respectively in our experimental conditions, and they are shown in Fig.12. The critical diameters for nucleous formation of Nb, Si and Al were estimated to be 0.5, 0.5 and 0.6nm respectively(8). The growth mechanism of particles was analysed by "Collision-Coalescence theory" based on "Free Molecule theory"(11). The relation between the time from nucleation initiation and the particle diameter was obtained by assuming the cooling velocity. The growth time was 10^{-1}-10^{-2}s and the particle diameter was about 10nm in case of the cooling velocity of 10^4-$10^5 deg.s^{-1}$.

Supposing the mixture of Nb and Al with the atomic ratio of 3:1 is supplied at $0.1g \cdot min^{-1}$, or $0.2g \cdot min^{-1}$, the diameters of Nb particles attain 7-18nm or 9-22nm during the cooling from 3000K to 2000K. Because the nucleation temperature of Al is lower than 2000K as described above, it may be difficult that Al dissolves into Nb particles. In fact the lattice constant of the UFP from the mixture of Nb and Al is not very different from that of Nb. Accordingly the solubility of Al in Nb is considered to be several % at most. There is a possibility that Al is coated on the surface of Nb particles. Nb_5Si_3 phase in the Nb-Si UFP is of W_5Si_3 type-a high temperature phase which is stable at temperatures over 2273K. From such consideration, it is concluded that the Nb-Si UFP may be formed at temperatures higher than 2273K. If the cooling velocity reaches $10^6 deg \cdot s^{-1}$, the diameters of Nb particles can be smaller than a few nm at the nucleation temperature of Al. So it may be possible to obtain Nb-Al alloy with a high content of dissolved Al.

CONCLUSIONS

Nb was detected in all UFP obtained from the mixture of Nb and Al by X-ray diffraction analysis. $NbAl_3$ was also detected in the UFP obtained from the mixture of Nb and Al in which Al concentration was higher than a certain value. Nb_5Si_3 phase of W_5Si_3 type was confirmed in the Nb-Si UFP obtained from the mixture of Nb and Si with the atomic ratio of 75:25.
The flow pattern, the temperature distribution and the cooling velocity of metal vapor in the plasma tail flame near the quenching region were estimated. The nucleation and growth mechanisms of the UFP could be analysed, referring to Lothe-Pound theory and Collision-Coalescence theory.

REFERENCES

(1) K.Kusaka, N.Wada and A.Tasaki, Japan J.Appl.Phys., 8, 599(1969).
(2) A.Iga and Y.Tawara, Japan J.Appl. Phys., 8, 1057(1969).
(3) Y.Fukano and K.Kimoto, J.Phys.Soc.J apan, 23, 668(1967).
(4) N.Yukawa et al, Trans.J.I.M., 9, 372(1968).
(5) Al Gal' and V V Gal', High Temp, High Press., 8, 255(1976).
(6) C.E.Lundin and A.S.Yamamoto, Trans.Metal.Soc.AIME, 236, 863(1966).
(7) C.J.Smithells,"Metal Reference Book", (Butterworths, London, 1976).
(8) T.Harada, A Master's Thesis,"Study of UFP syntheses of alloys by using rf induced plasma", The University of Tokyo(1981).
(9) R.T.V.Kung and S.H.Bauer, Proc.8th Shock Tube Symposium, London, 61(1971).
(10) J.Rothe and G.M.Pound, J.Chem.Phys., 36, 2080(1962).
(11) G.M.Hidy and J.R.Brock, J.Colloid Sci., 20, 477(1965).

Table 1. Experimental conditions (I)

reactor		(A)	(B)
gas flow rate(l/min)	inner working gas(Ar)	6.5	4
	(He)	2	3
	outer cooling gas(Ar)	40	30
	(H_2)	1-2	0
	carrier gas for powder feed(Ar)	4	3
supplied plate power (KVxA)		7x3.2	7.5x4.2
powder (Nb-Al) feeding rate (g/min)		0.16-0.19	~0.3

Table 2. Experimental conditions (II)

Apparatus	(C)					(D)					(C)
Atomic ratio of Nb:Al	3:1	2:1	1:1	1:2	1:3	3:1	2:1	1:1	1:2	1:3	3:1 (Nb:91)
Flow rate											
Ar(outside)	38.5	33	30	33	38	30	30	30	30	30	40
Ar(middle)	5.5	4.5	5	5	4.5	-	-	-	-	-	5
Ar(inside)	3	2	3	4	4	6	6	6	6	6	3
Ar(powder carrier)	2	1.8	2	3	2	3	3	3	3	3	3
He(inside)	5	0	0	5	4.5	1	1	1	1	1	5
H_2(outside)	1	0.5	1	1	2	1	1	1	1	1	4
Power											
E_p(KV)	8.5	8.1		8.4	8.4	6.7		6.5	6.5		8.5
I_p(A)	4.3	4.4		4.4	4.2	2.3		2.2	2.2		4
Supplying rate, powder (g/min)	0.21	0.11	0.09	0.08	0.13	0.08	0.11		0.04		0.33

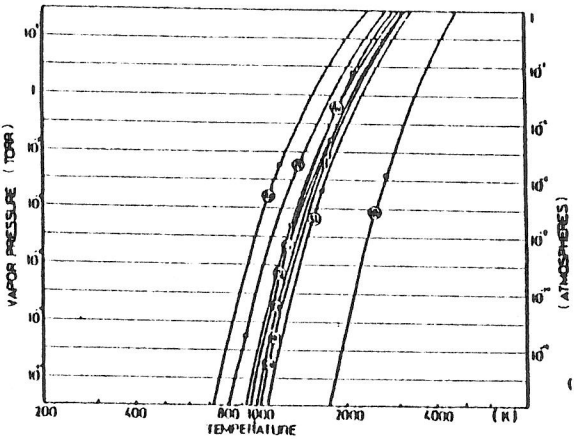

Fig.1. Vapor pressure vs. temperature in various metals.

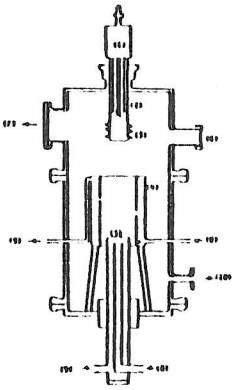

(1) Torch head
(2) Three concentric quartz tube
(3) rf coil
(4) Pyrex cylinder
(5) Cu quenching plate
(6) Window
(7) Connector to rf generator
(8) Water inlet
(9) Water outlet
(10) Gas outlet

Fig.2. Reactor(A)

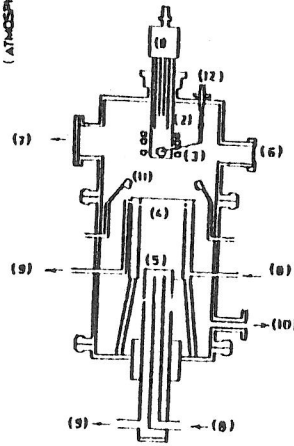

(1) Torch head
(2) Three concentric quartz tube
(3) RF coil
(4) Pyrex cylinder
(5) Cu quenching plate
(6) Window
(7) Connector to rf generator
(8) Water inlet
(9) Water outlet
(10) Gas outlet
(11) Gas quenching nozzle
(12) powder feeder

Fig.3. Reactor(B)

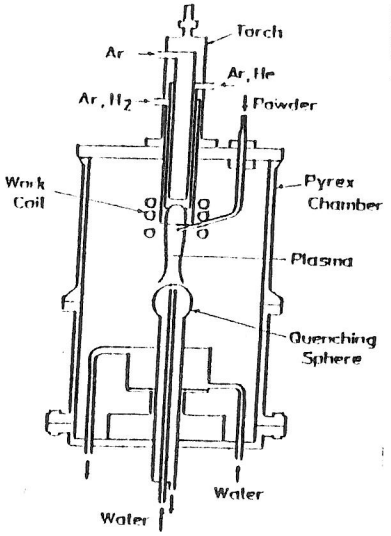

Fig.4. Reactor(C)

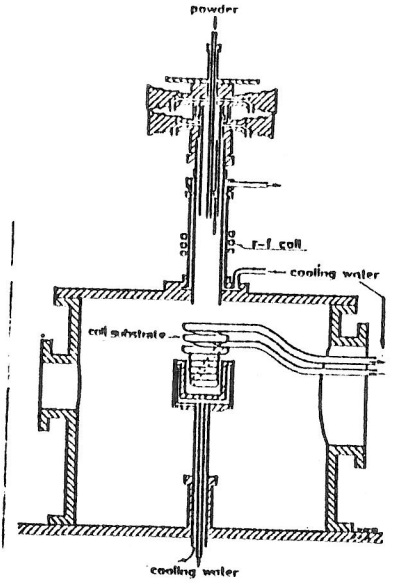

Fig.5. Reactor(D)

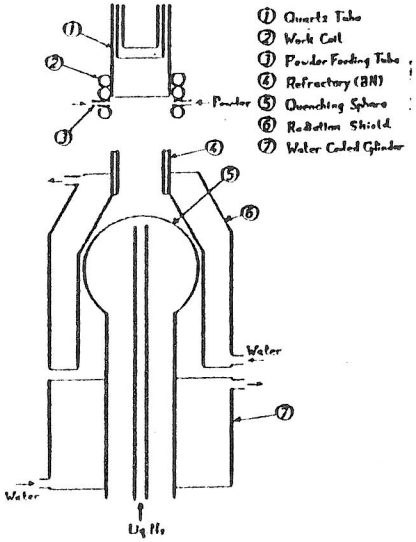

Fig.6. Quenching sphere with radiation shield.

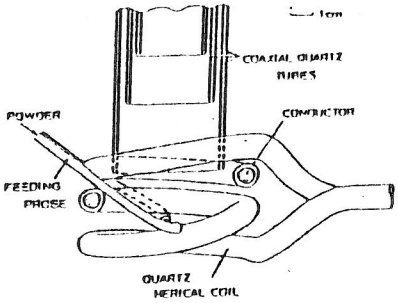

Fig.7. Detail of rf coil in reactor(C).

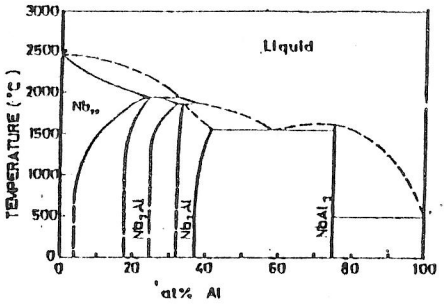

Fig.8. Phase diagram of Nb-Al.

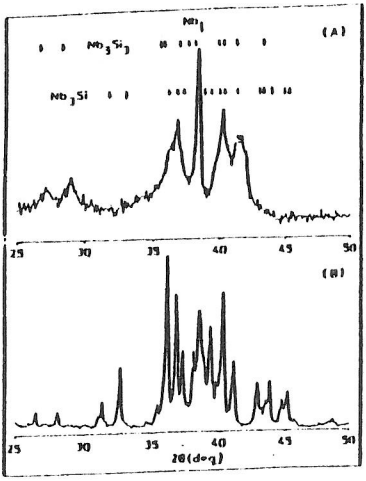

Fig.9. X-ray diffraction chart of Nb-Si(UFP).

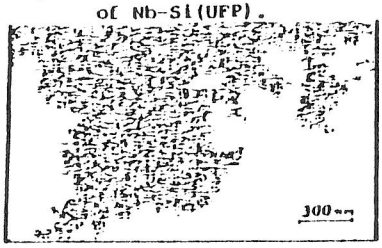

Fig.10. TEM of Nb-Al UFP.

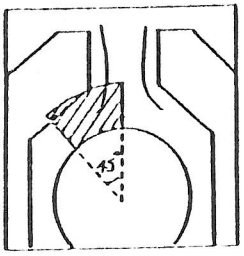

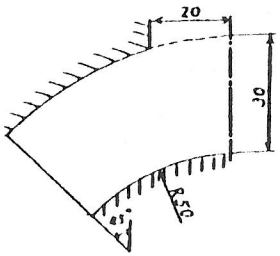

Fig.11. Dimension of sphere.

Table 3. X-ray diffraction analysis of Nb-Al (UFP).

MIX RATIO (Nb : Al)	DETECTED PHASES	
	EXP. A	EXP. B
3 : 1	Nb, NbH	Nb, NbH
2 : 1	Nb, NbH	Nb, NbH, $NbAl_3$, (Al)
1 : 1	Nb	Nb, NbH, $NbAl_3$, Al
1 : 2	Nb	Nb, $NbAl_3$, Al, (NbH)
1 : 3	Nb, $NbAl_3$	Nb, $NbAl_3$, Al

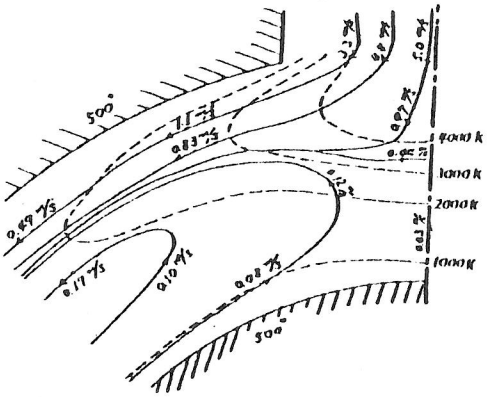

Fig.12. Flow pattern and temperature profile of plasma tail flame.

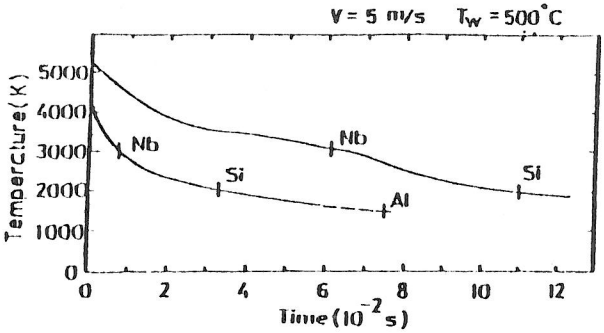

Fig.13. Cooling curves and nucleation temperatures of Nb, Si and Al.